Embedding theory for excited states with inclusion of self-consistent environment screening

Johannes Lischner and T.A. Arias

Laboratory of Atomic and Solid State Physics,
Cornell University, Ithaca, New York 14853

Dominika Zgid and Garnet Kin-Lic Chan

Department of Chemistry and Chemical Biology,
Cornell University, Ithaca, New York 14853

We present a general embedding theory of electronic excitations of a relatively small, localized system in contact with an extended, chemically complex environment. We demonstrate how to include the screening response of the environment into highly accurate electronic structure calculation of the localized system by means of an effective interaction between the electrons, which contains *only screening processes occurring in the environment*. For the common case of a localized system which constitutes an inhomogeneity in an otherwise homogeneous system, such as a defect in a crystal, we show how matrix elements of the environment-screened interaction can be calculated from density-functional calculations of the *homogeneous* system *only*. We apply our embedding theory to the calculation of excitation energies in crystalline ethylene.

I.   INTRODUCTION

Neutral electronic excited states play an important role in the study of condensed matter systems. They are probed in spectroscopic measurements, such as absorption, reflectivity or photoluminescence. In addition, they are important in many technical applications, such as photovoltaics, laser technology or light-emitting diodes. It is therefore necessary to develop a theoretical understanding of neutral electronic excitations.

Various theoretical approaches to calculating excited state properties have been developed in the past, each of which usually is applicable to certain classes of physical systems. Highly accurate quantum chemistry methods, such as configuration interaction or coupled cluster theory, can only be applied to small systems containing few electrons, such as atoms or small molecules. For larger molecules and clusters, time-dependent density-functional theory [1, 2] yields a reliable description of excited states. Many-body perturbation theory, where neutral excitation energies and oscillator strengths are obtained by solving the Bethe-Salpeter equation for the two-particle Green function,

constitutes a standard tool for neutral excited states in extended periodic systems, but has also been applied successfully to localized systems, such as molecules [3–5]. However, many-body perturbation theory, while being applicable to much larger systems than the quantum chemistry methods, still scales quite unfavorably with system size and often further approximation, such as model dielectric functions, are introduced when studying chemically complex crystals [6, 7].

Often, in extended systems one can identify a subsystem, which is of particular interest: for example, an adsorbed molecule near a solid surface or a defect in a crystal. In such systems, the electronic excitation is often localized on the special subsystem and a high level of accuracy is desired for the description of the excitation. However, while standard approaches for large systems, such as time-dependent density-functional theory, often do not yield the required accuracy, highly accurate quantum chemistry approaches can only be employed when the environment, which screens the potential created by the localized excitation, is ignored. Embedding theories, which attempt to combine a high-accuracy treatment of the subsystem with a more approximate treatment of the environment, attempt to overcome this difficulty. Those theories have a long history, but have focused mostly on ground-state properties [8].

Regarding excited state embedding, Whitten and coworkers [9] construct an embedding scheme, where a configuration interaction calculation of the subsystem is based on a Hartree-Fock calculation of a surrounding cluster. However, the description of the environment by a cluster is a severe approximation, which neglects long range screening effects. Carter and coworkers [10–14] building on previous work[15, 16] embed a configuration interaction calculation into an environment described by density-functional theory. Starting from a formally exact set of equations, Carter and coworkers [10] compute excitation energies of the subsystem by introducing an additional "external" potential due to the environment into their quantum chemistry calculation. However, they assume that the electron density of the environment in the excited state remains the same as in the ground state, neglecting the rearrangement of the environment electrons due to the excitation of the subsystem.

In this work, we present a theory of electronic excitations of a localized system in contact with an extended, chemically complex environment taking proper account of the environment response to the excitation on the localized system. In particular, we include the environment response through a special screened interaction, which contains only screening processes of the environment, acting between electrons of the subsystem. This environment-screened interaction is obtained by first carrying out density-functional calculations of the *homogeneous* system, e.g. the defect-free crystal, and then subtracting out screening processes due to the region which is replaced by the

explicit system (e.g. defect).

Once obtained, the environment-screened interaction can be used in various electronic structure methods for the localized, "explicit" system: we demonstrate how to include the environment response into a Green function calculation of the subsystem or into a wavefunction calculation.

This paper is organized as follows: in Section 1, we introduce the concept of an environment-screened interaction and describe its use in an embedding procedure, where the explicit region is treated by Green function methods. In Section 2, we describe the application of our embedding approach to wavefunctions methods, which are typically employed in quantum chemistry calculations. In particular, we introduce a self-consistent equation for the environment-screened potential caused by an external charge distribution and consequently transform this equation into a matrix form. We also discuss numerical difficulties of our embedding approach which are caused by (i) the divergence of the screened interaction and (ii) the extreme narrowness of the basis functions used in quantum chemistry. The first problem is solved by introducing a new integration scheme for integrals over the Brillouin zone, which avoids the approximations made in similar approaches. The second difficulty is overcome by computing the *changes* of the interaction matrix elements due to the presence of the environment, which can be evaluated efficiently in Fourier space because only the smooth parts of the basis functions are screened. In Section 3, we apply our theory to crystalline ethylene and discuss the effects of the crystalline environment on the excited states of these materials. Section 4 offers discussions and outlook.

II.   EMBEDDING THEORY AND APPLICATION GREEN FUNCTION METHODS

The identification of a localized subsystem, on which the modeling effort is concentrated, marks the starting point in every embedding approach. In our embedding approach for excited states, the physical system under consideration is divided into two regions: a localized "explicit" region, where the excitation occurs, and the rest of the system, the environment, which screens the potential created by the excitation. Having identified the relevant subsystem, we employ highly accurate, but computationally demanding electronic structure methods, such as the Green function methods or wavefunction methods, to describe the localized excitation. To include the influence of the environment into these calculations, we modify the interaction between the electrons to contain all screening processes occurring in the environment. This environment-screened interaction is obtained from less demanding many-body Green's function methods, evaluated eventually with the Kohn-Sham orbitals from density-functional theory calculations.

A.   Environment-screened interaction

The environment-screened interaction between electrons of the localized system, where the excitation occurs, plays a crucial role in our embedding approach. Quite often, it is possible and advantageous to replace a complicated calculation of a self-consistent environment response by the use of an effective or screened interaction, the simplest case being the interaction of two point charges in a linear dielectric medium. The notion of a screened interaction also plays an important role in quantum many-body theory, where Feynman diagrams are used to organize and gain intuition about the plethora of possible screening processes. Here we also employ a diagrammatic approach to derive an explicit expressions for the environment-screened interaction.

The rules for converting Feynman diagrams into algebraic expressions can be found in many textbooks, e.g. Ref. [17, 18]. In the diagrams below, dotted lines denote bare Coulomb interactions, while the fully screened (containing screening processes from the environment *and* the localized subsystem) interaction is represented by double-dotted lines. As usual, electron (and holes) are denoted by regular lines. The screened interaction is given by

$$
\text{(diagram)} \tag{1}
$$

By introducing the irreducible polarizability, represented below by a dashed square, we can express the infinite sum by a self-consistent Dyson equation. The irreducible polarizability contains all diagrams which cannot be separated into two parts by cutting a single dotted line. Dyson's equation for the screened interaction is given by

$$
\text{(diagram)} \tag{2}
$$

Of course, the exact form of the irreducible polarizability is unknown and must be approximated. A well-known approximation, which has proven extremely useful in many applications of electronic structure theory, is the random-phase approximation (RPA), where only simple electron-hole bubbles are inserted into the dotted lines in Eq. (1).

The electron and hole of each bubble are either part of the explicit subsystem or part of the environment. In the following, Green function lines corresponding to subsystem electrons (and

holes) are colored red, environment electrons (and holes) are colored blue. Consequently, a diagram representing an electron-hole bubble gives rise to four colored diagrams

$$
\text{----} \bigcirc \text{----} \quad \rightarrow \quad \text{----} \bigcirc \text{----} \; , \; \text{----} \bigcirc \text{----} \; , \; \text{----} \bigcirc \text{----} \; , \; \text{----} \bigcirc \text{----} \; .
$$

(3)

In the first colored Feynman diagram an electron-hole pair is created in the environment, while in the second diagram the pair is created in the explicit region. In the third and fourth diagrams one particle is created in the environment, while the other is created in the explicit system. The contribution to the total screening from such diagrams, where environment particle lines and system particle lines connect, is small if there is little wavefunction overlap between subsystem and environment. Algebraically, such an electron-hole bubble corresponds to the product of a Green function $G_{sys}(r, r')$ describing particles in the explicit system and a Green function $G_{env}(r, r')$ describing environment particles. Because the bare Green function is proportional $\psi(r)\psi^*(r')$, the product will vanish if environment and system wavefunctions do not overlap.

Within the RPA, the fully screened interaction can therefore be expressed as

$$
\text{=====} \; = \; \text{------} \; + \text{---} \bigcirc \text{---} \; + \text{---} \bigcirc \text{---} \; + \text{--} \bigcirc \text{--} \bigcirc \text{--} \; + \text{--} \bigcirc \text{--} \bigcirc \text{--} \; + \; ...
$$

(4)

We now define the environment-screened interaction, which is represented by a blue double-dotted line and contains only environment bubbles, according to

$$
\text{=====} \; = \; \text{------} \; + \text{---} \bigcirc \text{---} \; + \text{--} \bigcirc \text{--} \bigcirc \text{--} \; + \text{--} \bigcirc \text{--} \bigcirc \text{--} \bigcirc \text{--} \; + \; ... \quad (5)
$$

Note that the fully (within the RPA) screened interaction can be obtained from the environment-screened one via

$$
\text{=====} \; = \; \text{=====} \; + \text{====} \bigcirc \text{====} \; + \text{==} \bigcirc \text{==} \bigcirc \text{==} \; + \text{==} \bigcirc \text{==} \bigcirc \text{==} \bigcirc \text{==} \; + \; ...
$$

(6)

This simple result has important consequences: it allows us to rigorously replace the whole system, consisting of the localized subsystem and the environment, by an "effective" subsystem, in which electrons interact through the environment-screened interaction.

We note that this result is not limited to the random-phase approximation of the screened interaction, but is found quite generally whenever the irreducible polarizability is a sum of two pieces: one containing only environment electrons, the other only system electrons. This opens up the possibility of concentrating the modelling effort on the localized subsystem by using more sophisticated approaches for this region than the RPA. In our approach, we employ the RPA for the environment-screened interactions and use highly accurate electronic structure methods, such as Green function theory or explicit wavefunction approaches, for the localized subsystem.

B. Embedding in Green function methods

In this section, we demonstrate how to use the environment-screened interaction to construct an embedding theory, where the excitation on the localized system is described by Green function methods.

The Bethe-Salpeter equation of many-body perturbation theory solves for the dressed particle-hole Green function [2, 3], whose poles give the excitation energies of the system, and has been applied successfully to extended periodic systems, but also clusters and molecules [3, 4].

Diagrammatically, the Bethe-Salpeter equation is given by

$$\tag{7}$$

where the term in parenthesis represents the Bethe-Salpeter approximation to the self-energy of the particle-hole Green function and contains an unscreened exchange interaction and a fully screened direct interaction. Typically, the fully screened interaction is obtained from the static dielectric matrix within the random-phase approximation [2, 3].
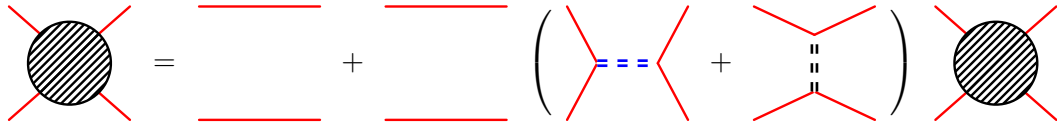
To obtain an embedding theory within the Bethe-Salpeter framework, we again color the electron lines red for system electrons and blue for environment electrons. Assuming that the exciton is localized in the explicit region, we impose that the incoming and outgoing lines in Eq. (7) are red system lines. The direct interaction already is fully screened containing the screening contributions from both the localized system and the environment. However, expressing the self-consistent Bethe-Salpeter equation (Eq. (7)) by an infinite sum of diagrams, we observe that the exchange interaction

in the two-particle self-energy gives rise to diagrams like

$$\tag{8}$$

To capture such an exchange-type process, where a particle-hole pair of the localized system anni-
hilates and re-emerges after creating an intermediate electron-hole pair in the environment, in our
embedding approach, we replace the bare exchange diagram in Eq. (7) by an environment-screened
exchange.

It is easy to verify that the following Bethe-Salpeter equation for the embedded system

$$\tag{9}$$

indeed gives rise to diagrams like Eq. (8).

However, apart from the aforementioned embedding approximations (neglect of diagrams with
environment lines connecting into system lines and the assumption that the exciton resides on the
explicit system), the proposed embedded Bethe-Salpeter equation contains one further approxima-
tion: all environment bubbles are empty, i.e. diagrams like
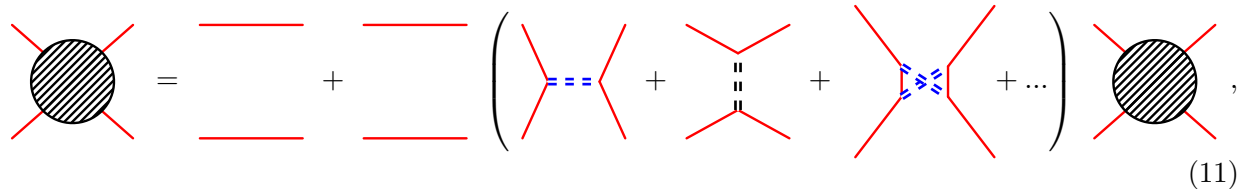

$$\tag{10}$$

which can be constructed from Eq. (7), are absent in Eq. (9). In these diagrams, additional
interactions between electron-hole pairs of the environment are included. Nevertheless, we expect
that Eq. (9) captures the vast majority of all screening processes.

Computationally, the embedded Bethe-Salpeter equation has the advantage that, once the
environment-screened interaction is computed, Eq. (9) can be conveniently solved in a localized
basis, such as gaussians [3], with relatively few basis functions.

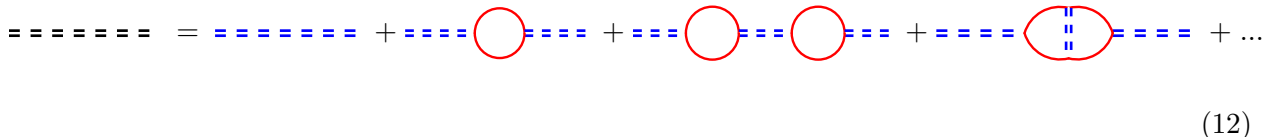### III.   EMBEDDING IN WAVEFUNCTION METHODS

Having introduced the general notion of an environment-screened interaction and having seen
its use in an embedded Bethe-Salpeter equation, we now move on to embed a localized system
described by wavefunction methods, which are typically used in quantum chemistry calculations,
into an environment described by the random phase approximation of many body theory.

We use the Lehmann representation of the particle-hole Green function [19] to connect the many-body wavefunctions and the corresponding eigenenergies to the diagrammatic Green function formulation of the last section. Thus, we may view the result of a full configuration interaction calculation as the solution of a generalized Bethe-Salpeter equation with the *exact* two-particle self-energy for the electrons of the localized subsystem. Diagrammatically, this corresponds to

$$\tag{11}$$

where the term in brackets now contains more complicated irreducible diagrams. Also, the fully screened interaction is not given by Eq. (6) any more, but contains more complicated screening processes due to the exact treatment of the subsystem

$$\tag{12}$$

Again, the use of the environment-screened interaction in wavefunction methods allows for the application of these methods to large systems containing many electrons, which traditionally are out of reach for these methods. In addition to the environment-screened interaction, which only describes response properties of the environment, we note that it is also necessary to include an additional external potential into the quantum chemistry calculation, which is caused by the ground state configuration of the environment.

A. Self-Consistent Equations for Environment-Screened Potential

Having demonstrated the usefulness of an environment-screened interaction for excited state embedding approaches, we now turn to the task of computing it. While the calculation of the fully screened interaction is relatively straightforward in localized or periodic systems, the calculation of the interaction with *only* environment screening proves more difficult if the localized system constitutes an inhomogeneity in an otherwise homogeneous system, such as a defect in a crystal. For this case, we demonstrate how matrix elements of the environment-screened interaction can be calculated from random phase approximation calculations of only the *homogeneous* system

(crystal without defect) by subtracting out screening contributions from the region where the inhomogeneity (defect) resides. The desired matrix elements are computed from the environment-screened *potential* resulting from the "external charge density" of a product of basis functions. This potential obeys a self-consistent equation introduced in this section, which - in the next section - is then transformed into a matrix form.

After choosing an explicit set of basis functions g_i (assumed to be real) for the quantum chemistry calculation of the embedded localized subsystem, the interaction $v(\mathbf{r}, \mathbf{r}')$ between electrons appears in the resulting matrix form of Schroedinger's equation only in interaction matrix elements of the form

$$\langle g_1, g_2 | v | g_3, g_4 \rangle = \int d^3 r \int d^3 r' g_1(\mathbf{r}) g_2(\mathbf{r}) v(\mathbf{r}, \mathbf{r}') g_3(\mathbf{r}') g_4(\mathbf{r}'). \tag{13}$$

In our embedding approach, we replace the bare Coulomb potential $\Phi(\mathbf{r}) = \int d^3 r' g_3(\mathbf{r}') g_4(\mathbf{r}') / |\mathbf{r} - \mathbf{r}'|$ due to the "charge distribution" $g_3 g_4$ in Eq. (13) by the environment-screened potential $\tilde{\Phi}$ according to

$$\langle g_1, g_2 | \Phi \rangle \rightarrow \langle g_1, g_2 | \tilde{\Phi} \rangle. \tag{14}$$

$\tilde{\Phi}$ takes into account the response of all environment molecules to the "external charge density" $\rho_{ext} = g_3 g_4$ and solves the self-consistent equation

$$\tilde{\Phi} = K(\rho_{ext} + \chi_{env} \tilde{\Phi}), \tag{15}$$

where K denotes the bare Coulomb operator $[K\rho](\mathbf{r}) = \int d^3 r' \rho(\mathbf{r}') / |\mathbf{r} - \mathbf{r}'|$ and $\chi_{env} = \chi_{crys} - \chi_{sys}$ is the environment polarizability given by the difference of the polarizability of the full crystal (without the inhomogeneity) and the polarizability of the local subsystem. We note that $\chi_{env} \tilde{\Phi}$ is the self-consistent induced charge density in the environment caused by the external charge ρ_{ext}.

Solution of Eq. (15) is complicated by the presence of both quantities that describe extended systems and are best represented in Fourier space, such χ_{crys}, and quantities which describe the explicit local system and are best represented by localized functions, such as χ_{sys}. We overcome this difficulty by replacing solution of Eq. (15) by a two step process: In the first step, we compute the effective field due to an external charge ρ_{tot} allowing the whole crystal (and not only the environment region) to screen the external charge. Consequently, $\tilde{\Phi}$ obeys

$$\tilde{\Phi} = K(\rho_{tot} + \chi_{crys} \tilde{\Phi}). \tag{16}$$

Expressing all quantities in plane waves, this equation can be solved straightforwardly yielding

$$\tilde{\Phi} = (K^{-1} - \chi_{crys})^{-1} \rho_{tot} \equiv K_{crys} \rho_{tot}, \tag{17}$$

where K_{crys} denotes the fully screened interaction of the homogeneous system (e.g. perfect crystal without defect).

In the second step, we impose that the total external charge in Eq. (16) must be given by

$$\rho_{tot} = \rho_{ext} + \Delta\rho = \rho_{ext} - \chi_{sys}\tilde{\Phi}, \tag{18}$$

which involves only the localized system response and can be solved in a localized representation. Inserting Eq. (18) into Eq. (16) clearly gives back Eq. (15). Alternatively, we can substitute Eq. (17) into Eq. (18) yielding

$$\Delta\rho = -\chi_{sys}K_{crys}\rho_{tot} = -\chi_{sys}K_{crys}(\rho_{ext} + \Delta\rho), \tag{19}$$

which now constitutes a self-consistent equation for $\Delta\rho$. In the following, we will make use of this latter equation.

B. Transformation to matrix equation

We now show how to transform Eq. (19) for the charge density $\Delta\rho$ induced in the environment into a matrix equation.

We employ the random-phase approximation for the polarizability of the explicit system

$$\chi_{sys}(\mathbf{r}, \mathbf{r}'|\omega) = 2\sum_{jk}(f_k - f_j)\frac{\phi_k^*(\mathbf{r})\phi_j(\mathbf{r})[\phi_k^*(\mathbf{r}')\phi_j(\mathbf{r}')]^*}{\omega - (\epsilon_j - \epsilon_k) + i\eta}, \tag{20}$$

where $f_i = 0$ or 1 are occupation factors, $\phi_i(\mathbf{r})$ and ϵ_i denote single-particle wavefunctions and orbital energies of the local system, respectively. From now on, we will work in the static approximation setting $\omega = 0$, which is well-justified for many applications [20].

Introducing the standard transition-space notation, where the transition of an electron from orbital k to orbital j is labeled by $\mu = (k, j)$, we express χ_{sys} as

$$\chi_{sys}(\mathbf{r}, \mathbf{r}') = \sum_{\mu=(v,c)} \rho_\mu(\mathbf{r})\chi_\mu\rho_\mu^*(\mathbf{r}'), \tag{21}$$

with $\chi_\mu = 4/(\epsilon_j - \epsilon_k)$, $\rho_\mu(\mathbf{r}) = \phi_k^*(\mathbf{r})\phi_j(\mathbf{r})$ and the indices v and c run over occupied and empty orbitals, respectively. Inserting this expression for χ_{sys} into Eq. (19) yields

$$\Delta\rho(\mathbf{r}) = -\sum_\mu \rho_\mu(\mathbf{r})\chi_\mu \int d^3r' \int d^3r'' \rho_\mu^*(\mathbf{r}')K_{crys}(\mathbf{r}', \mathbf{r}'')[\rho_{ext}(\mathbf{r}'') + \Delta\rho(\mathbf{r}'')]. \tag{22}$$

The ansatz $\Delta\rho(\mathbf{r}) = \sum_\mu A_\mu \rho_\mu(\mathbf{r})$ then leads to the following matrix equation for the coefficients A_μ

$$A_\mu = -\chi_\mu \left(a_\mu + \sum_\nu M_{\mu\nu} A_\nu \right), \tag{23}$$

where we defined

$$a_\mu = \int d^3r \int d^3r' \rho_\mu^*(\mathbf{r}) K_{crys}(\mathbf{r}, \mathbf{r}') \rho_{ext}(\mathbf{r}'), \tag{24}$$

$$M_{\mu\nu} = \int d^3r \int d^3r' \rho_\mu^*(\mathbf{r}) K_{crys}(\mathbf{r}, \mathbf{r}') \rho_\nu(\mathbf{r}'). \tag{25}$$

Solving Eq. (23) we arrive at

$$A = -[\chi^{-1} + M]^{-1} a, \tag{26}$$

with $\chi_{\mu\nu}^{-1} = \chi_\mu^{-1} \delta_{\mu\nu}$. In sum, we solved Eq. (19) for $\Delta\rho$ in terms of the transition-space matrix M and the vector a, which involve the fully screened interaction K_{crys} of the corresponding homogeneous system. In the next section, we describe how these quantities are computed within the random-phase approximation.

C. Calculation of M and a

Exploiting the translational symmetry of the crystal without the inhomogeneity (i.e. the localized subsystem), we express K_{crys}, ρ_{ext} and ρ_μ as integrals over the Brillouin zone. For example, ρ_μ is given by

$$\rho_\mu(\mathbf{r}) = \int_{BZ} \frac{d^3q}{V_{BZ}} \rho_{\mu,\mathbf{q}}(\mathbf{r}) e^{i\mathbf{q}\cdot\mathbf{r}}, \tag{27}$$

where $V_{BZ} = (2\pi)^3/V_{cell}$ denotes the volume of the Brillouin zone with V_{cell} being the unit cell volume. We note that $\rho_{\mu,\mathbf{q}}(\mathbf{r}) = \sum_{\mathbf{G}} \rho_{\mu,\mathbf{q}}(\mathbf{G}) \exp(i\mathbf{G}\cdot\mathbf{r})$, where $\mathbf{G}$ denotes a reciprocal lattice vector, is a lattice-periodic function.

To compute K_{crys} [Eq. (17)], the polarizability of the crystal is taken in the static random-phase approximation [21, 22] and explicitly given by

$$\chi_{crys,\mathbf{q}}(\mathbf{G}, \mathbf{G}') = \frac{4}{N_q V_{cell}} \sum_{cv\mathbf{k}} \frac{\langle v,\mathbf{k}|e^{-i(\mathbf{q}+\mathbf{G})\cdot\mathbf{r}}|c,\mathbf{k}+\mathbf{q}\rangle \langle c,\mathbf{k}+\mathbf{q}|e^{i(\mathbf{q}+\mathbf{G}')\cdot\mathbf{r}'}|v,\mathbf{k}\rangle}{\epsilon_{v,\mathbf{k}} - \epsilon_{c,\mathbf{k}+\mathbf{q}}}, \tag{28}$$

where N_q is the number of sample points in the Brillouin zone and the indices c and v run over conduction and valence states, respectively. In the molecular crystals we are interested in orbitals

on neighboring molecules overlap very little, allowing for additional simplifications: (i) we assume flat bands, i.e. $\epsilon_{n,\mathbf{k}} = \epsilon_n$, and (ii) we assume that the crystalline Bloch states can be constructed from the wavefunction at the Γ-point through a tight-binding procedure via

$$\phi_{n\mathbf{k}}(\mathbf{r}) = \frac{1}{\sqrt{N_q}} \sum_{\mathbf{R}} e^{i\mathbf{k}\cdot\mathbf{R}} w_n(\mathbf{r} - \mathbf{R}), \tag{29}$$

where $\mathbf{R}$ runs over all N_q units cells comprising the crystal and $w_n(\mathbf{r}) = \psi_{n\mathbf{k}=0}(\mathbf{r})$ in the unit cell surrounding the origin and $w_n(\mathbf{r}) = 0$ in all other cells. Formally, Eq. (29) describes the Wannier transformation from localized orbitals or Wannier functions to Bloch states using an approximate Wannier function w_n [note that the exact Wannier function is given by $w_{n\mathbf{R}} = 1/\sqrt{N_q} \times \sum_{\mathbf{k}} \exp(-i\mathbf{k}\cdot\mathbf{R})\psi_{n\mathbf{k}}$].

The tight-binding ansatz eliminates the summation over the Brillouin zone in Eq. (28) and yields

$$\chi_{crys,\mathbf{q}}(\mathbf{G}, \mathbf{G}') = \frac{4}{V_{cell}} \sum_{vc} \langle v|e^{-i(\mathbf{q}+\mathbf{G})\cdot\mathbf{r}}|c\rangle \frac{1}{\epsilon_v - \epsilon_c} \langle c|e^{i(\mathbf{q}+\mathbf{G}')\cdot\mathbf{r}'}|v\rangle, \tag{30}$$

where $\langle v|e^{-i(\mathbf{q}+\mathbf{G})\cdot\mathbf{r}}|c\rangle = \int_{V_{cell}} d^3r \phi_v^*(\mathbf{r}) e^{-i(\mathbf{q}+\mathbf{G})\cdot\mathbf{r}} \phi_c(\mathbf{r})$. We point out that the tight-binding approximation for the crystal polarizability is invoked only for numerical convenience and that all following expressions can also be evaluated using the full RPA polarizability, given in Eq. (28), instead.

Finally, we express K_{crys} in terms of the symmetrized dielectric matrix $\tilde{\epsilon}_{\mathbf{q}}(\mathbf{G}, \mathbf{G}') = \delta_{\mathbf{G}\mathbf{G}'} - K_{\mathbf{q}}^{1/2}(\mathbf{G})\chi_{crys,\mathbf{q}}(\mathbf{G}, \mathbf{G}')K_{\mathbf{q}}^{1/2}(\mathbf{G}')$ via

$$K_{crys,\mathbf{q}}(\mathbf{G}, \mathbf{G}') = K_{\mathbf{q}}^{1/2}(\mathbf{G})\tilde{\epsilon}_{\mathbf{q}}^{-1}(\mathbf{G}, \mathbf{G}')K_{\mathbf{q}}^{1/2}(\mathbf{G}'), \tag{31}$$

with $K_{\mathbf{q}}(\mathbf{G}) = 4\pi/|\mathbf{q} + \mathbf{G}|^2$. The components of M and a can now be expressed completely in Fourier space and are given by

$$a_\mu = V_{cell} \int \frac{d^3q}{V_{BZ}} \sum_{\mathbf{G}\mathbf{G}'} \rho_{\mu,\mathbf{q}}^*(\mathbf{G}) K_{crys,\mathbf{q}}(\mathbf{G}, \mathbf{G}') \rho_{ext,\mathbf{q}}(\mathbf{G}'), \tag{32}$$

$$M_{\mu\nu} = V_{cell} \int \frac{d^3q}{V_{BZ}} \sum_{\mathbf{G}\mathbf{G}'} \rho_{\mu,\mathbf{q}}^*(\mathbf{G}) K_{crys,\mathbf{q}}(\mathbf{G}, \mathbf{G}') \rho_{\nu,\mathbf{q}}(\mathbf{G}'). \tag{33}$$

D. Environment-screened interaction matrix element

The final expression for the environment-screened matrix element is

$$
\begin{aligned}
\langle g_1, g_2 | \tilde{\Phi} \rangle &= \langle g_1, g_2 | K_{crys} | \rho_{ext}(3,4) + \Delta\rho(3,4) \rangle \\
&= \langle g_1, g_2 | K_{crys} | g_3, g_4 \rangle + \langle g_1, g_2 | K_{crys} | \sum_{\mu} A_{\mu}(3,4) \rho_{\mu} \rangle \\
&= \langle g_1, g_2 | K_{crys} | g_3, g_4 \rangle - a^{\dagger}(1,2) X a(3,4),
\end{aligned}
\tag{34}
$$

where we defined $X = [\chi^{-1} + M]^{-1}$ and we used Eqs. (17), (18) and (26). We also now explicitly write $a(3,4)$ to denote explicitly the dependence on the basis functions g_i (similarly for $\Delta\rho$ and A).

E. Numerical challenges

In this section, we discuss the two major numerical difficulties of the described embedding approach: (i) the integrations over the Brillouin zone in Eqs. (32) and (33) and (ii) the handling of extremely narrow basis functions.

Regarding the first issue, we note that the Brillouin zone integrals in Eqs. (32) and (33) must be handled with great care, because certain elements of $K_{crys,\mathbf{q}}$ diverge as $|\mathbf{q}|$ approaches zero: the head $K_{crys,\mathbf{q}}(0,0)$ diverges as $1/\mathbf{q}^2$ and the wings, $K_{crys,\mathbf{q}}(0, \mathbf{G}')$ and $K_{crys,\mathbf{q}}(\mathbf{G}, 0)$, diverge as $1/|\mathbf{q}|$. Although these singularities are integrable, they can cause extremely slow convergence when the integral is approximated by a discrete sum over sample points in the Brillouin zone.

Most approaches [23, 24] use a regular mesh including the origin to carry out the Brillouin zone integration. The contribution from the volume element at the origin is obtained by approximating the smooth part of the integrand by its value at the origin, replacing the volume element by a sphere of equal volume and finally analytically integrating the divergent part of the integrand in the spherical volume. While numerically efficient, we expect the error associated with this scheme to converge quite slowly. Also, in anisotropic systems the smooth part of the integrand might not even be well-defined at the origin and instead vary strongly depending on the direction of approach towards the origin.

In contrast, in our approach we first isolate the singular parts of the integrand by splitting the integral over the Brillouin zone into two parts. The part containing the singularity is transformed to spherical coordinates thus removing the singularity, while the other part is evaluated using a

regular grid over the Brillouin zone. For a generic function $f(\mathbf{q})$, we write

$$\int d^3q f(\mathbf{q}) = \int d^3q (1 - e^{-\sigma^4 \mathbf{q}^4}) f(\mathbf{q}) + \int d^3q e^{-\sigma^4 \mathbf{q}^4} f(\mathbf{q}), \tag{35}$$

where σ is a parameter which can be adjusted to optimize convergence. Note that the integrand in the first term on the right hand side is well-behaved at the origin, even if $f(\mathbf{q})$ diverges as $1/\mathbf{q}^2$. We use a simple regular grid over the whole Brillouin zone to evaluate this term. The integrand of the second term is divergent at the origin if $f(\mathbf{q})$ diverges, but vanishes rapidly as $|\mathbf{q}|$ increases because of the fast decay of $\exp(-\sigma^4 \mathbf{q}^4)$. The singularity can be removed by transforming the integral to spherical coordinates yielding

$$\int d^3q e^{-\sigma^4 \mathbf{q}^4} f(\mathbf{q}) = \int dq \left(q^2 e^{-\sigma^4 q^4} \int d\Omega f(q, \Omega) \right), \tag{36}$$

where the integrand in parentheses is now well-behaved at the origin and relatively smooth, such that we can use a Gaussian quadrature scheme for accurate evaluation. We also use Gaussian quadrature to carry out the integral over spherical angles.

Our scheme thus avoids the approximations described above. In particular, the contribution from the singular region surrounding the origin is computed with high accuracy. Also, the smooth part of the integrand is never evaluated at the origin, where it is not necessarily uniquely defined, making our scheme ideal for the study of anisotropic systems.

Regarding the second issue raised above, the difficulty of handling extremely narrow basis functions, we point out that, in actual density-functional calculations, the Kohn-Sham orbitals are represented on discrete real-space or Fourier space grids, which are typically too coarse to faithfully represent the narrow basis functions used in quantum chemistry calculations. However, because the crystal polarizability [Eq. (28)] entering the fully screened interaction is computed from Kohn-Sham orbitals only Fourier components of the "external charge density" (caused by a pair of basis functions) which belong to the grid of the density-functional calculation are screened, suggesting that the crystal-screened interaction can be decomposed as

$$K_{crys} = K + \Delta K_{crys}, \tag{37}$$

where ΔK_{crys} now only acts on the space of functions representable on the grid of the density-functional calculation. Instead of the full environment-screened interaction matrix element [Eq. (34)], the calculation of which would require grids fine enough to represent the narrow basis functions, we compute the difference $\langle g_1 g_2 | \Delta K_{crys} | g_3 g_4 \rangle$, which allows us to work with the grids of the density-functional calculation only. This difference has to be added to the bare Coulomb matrix element, which is computed with high accuracy in existing quantum chemistry codes.

F. External potential due to environment

In addition to the environment-screened interaction, we also include a static external potential caused by the ground state configuration of the environment into the quantum chemistry calculation. The inclusion of this additional external potential is necessary, because the environment-screened interaction only accounts for *response effects* in the environment, but not for the *static effect of the environment ground state configuration* on the electrons of the localized subsystem. The proper definition of the external potential requires great care in order to avoid "double counting" of interaction processes between the explicit system and the environment.

To reproduce the correct change in electron density $\delta\rho$ in the localized system system upon embedding, the external potential ϕ_{ext} must fulfill

$$\delta\rho = \chi_{scr}\,\phi_{ext}, \tag{38}$$

where χ_{scr} denotes the response function of the localized subsystem with an environment-screened interaction between the electrons and we assumed that ϕ_{ext} is relatively weak. If the wavefunction overlap between subsystem and environment is small, we can relate ϕ_{ext} to the total electrostatic potential ϕ_{env} due to the environment ground state configuration. ϕ_{env} is given by

$$\phi_{env} = K\rho_{env}, \tag{39}$$

where the environment charge density ρ_{env} is the sum of electronic and nuclear contributions. From its definition, ϕ_{env} produces the correct change in density $\delta\rho$, when applied to the subsystem with *unscreened interactions* between the electrons. If the potential is weak, this implies

$$\delta\rho = \chi_0\,\phi_{env}, \tag{40}$$

where χ_0 denotes the response function of the subsystem with unscreened interactions. Combining Eq. (38) and Eq. (40), we find

$$\phi_{ext} = \chi_{scr}^{-1}\,\chi_0\,\phi_{env}, \tag{41}$$

which allows for the calculation of the correct external potential from the electrostatic potential caused by the environment ground state configuration.

IV. APPLICATION TO ORGANIC CRYSTALS

In this section, we apply the described embedding approach to study electronic excitations in crystals consisting of short organic molecules. In these crystals, we take the molecules of a single

unit cell as the localized subsystem and all other molecules as the environment.

As a test case, we investigate crystalline ethylene. Crystalline ethylene being one of the simplest organic molecular crystals has been studied for a long time[25–27].

The excitations of isolated short organic molecules have attracted considerable attention because of the non-trivial character of their low-lying excited states [28–30]. For example, contrary to naive expectations the lowest excited state of the octatetraene molecule is not a one-electron (HOMO-LUMO) excitation, but has a $HOMO^2$-$LUMO^2$ double-excitation character [29, 30].

Upon embedding the molecule in a crystalline environment, we expect the molecular excitations to be altered because of (i) the screening by the crystalline environment and (ii) the delocalization of the excited state over several neighboring molecules. For crystals of short acenes, Ambrosch-Draxl and coworkers [31] found that there is very little delocalization of the excitation. We therefore only include the two inequivalent molecules of a single unit cell into our embedded quantum-chemistry calculation.

A. Computational details

We carry out density-functional calculations of ethylene crystals using the generalized gradient approximation [32]. We employ Kleinman-Bylander pseudopotentials [33], a plane wave cutoff of 40 Hartree and a $2 \times 2 \times 2$ Monckhorst-Pack [34] kpoint grid. For ethylene, the crystal structure is well-known from x-ray and neutron diffraction and we employ the lattice parameters and atomic positions provided by Ref. [35] in our calculation. We then relax the ionic positions and compute a large number of empty bands, which are needed for the calculation of the polarizability [Eq. (20)].

Next, we evaluate the environment-screened interaction matrix elements, Eq. (33). In this calculation, we only employ a subset of the reciprocal lattice used in the density-functional calculations consisting of ~ 1000 reciprocal lattice vectors. We find that the matrix elements are sufficiently converged if 200 empty bands are used. For the Brillouin zone summation, we employ a regular grid containing 512 kpoints for the first integral in Eq. (36) and 270 kpoints for the second integral, which contains the singularity. Finally, we approximate the external potential by the electrostatic potential of the environment, $\phi_{ext} \approx \phi_{env}$.

To compute excited states of the localized subsystem, we carry out configuration interaction calculations using the 6-31G basis set.

	bare [eV]	screened [eV]
state 1	17.432	17.384
state 2	17.436	17.554
state 3	19.004	19.004

TABLE I: Lowest excitations energies (measured from the ground state energy) in crystalline ethylene. The first column contains excitation energies obtained from configuration interaction calculations of the two molecules in a unit cell without any environment effects. The second column contains excitation energies for the unit cell embedded in the crystalline environment.

B. Results

Table I shows our results for the energies of lowest lying excitations in crystalline ethylene. We observe that the changes due to the environment screening are smaller than one percent. Interestingly, we find that the inclusion of environment screening lowers the energy of the lowest excited state, but increases the energy of the second lowest excited state. The energy of the third lowest excited state remains constant.

C. Discussion and Outlook

In this work, we have described a general framework for embedding theories of excited states in physical systems where the excitation is localized on a small subsystem. Contrary to previous approaches, we fully include the self-consistent screening response of the environment by using an effective interaction between electrons in the explicit subsystem. Once obtained, the environment-screened interaction may be employed in various highly accurate electronic structure description of the localized subsystem: we demonstrate how environment effects can be incorporated into Green function methods or wavefunction methods, which are typically employed in quantum chemistry.

We apply our embedding theory to the calculation of excited state energies of crystalline ethylene and find encouraging results.

[1] E. Runge and E. K. U. Gross, Phys. Rev. Lett. **52**, 997 (1984).

[2] G. Onida, L. Reining, and A. Rubio, Rev. Mod. Phys. **74**, 601 (2002).

[3] M. Rohlfing and S. G. Louie, Rev. Phys. B **62**, 4927 (2000).

[4] J. C. Grossman, M. Rohlfing, L. Mitas, S. G. Louie, and M. L. Cohen, Rev. Phys. Lett. **86**, 472 (2001).

[5] P. H. Hahn, W. G. Schmidt, and F. Bechstedt, Rev. Phys. B **72**, 245425 (2005).

[6] J.-W. van der Horst, P. A. Bobbert, M. A. J. Michels, and H. Baessler, J. Chem. Phys. **114**, 6950 (2001).

[7] J.-W. van der Horst, P. A. Bobbert, P. H. L. de Jong, M. A. J. Michels, G. Brocks, and P. J. Kelly, Phys. Rev. B **61**, 15817 (2000).

[8] P. Huang and E. A. Carter, Annu. Rev. Phys. Chem. **59**, 261 (2008).

[9] J. L. Whitten and H. Yang, Int. J. Quantum Chem. **56**, 41 (1995).

[10] P. Huang and E. A. Carter, J. Chem. Phys. **125**, 084102 (2006).

[11] N. Govind, Y. A. Wang, A. J. R. da Silva, and E. A. Carter, Chem. Phys. Lett. **295**, 129 (1998).

[12] N. Govind, Y. A. Wang, and E. A. Carter, J. Chem. Phys. **110**, 7677 (1999).

[13] T. Kluener, N. Govind, Y. A. Wang, and E. A. Carter, Phys. Rev. Lett. **88**, 209702 (2001).

[14] T. Kluener, N. Govind, Y. A. Wang, and E. A. Carter, J. Chem. Phys. **116**, 42 (2002).

[15] P. Cortona, Phys. Rev. B **44**, 8454 (1991).

[16] T. A. Wesolowski and A. Warshel, J. Phys. Chem. **97**, 8050 (1993).

[17] G. D. Mahan, *Many-Particle Physics* (Plenum Press, New York and London, 1981).

[18] A. L. Fetter and J. D. Walecka, *Quantum Theory of Many-Particle Systems* (Dover Publications, Inc., Mineola, New York, 1971).

[19] G. Strinati, Phys. Rev. B **29**, 5718 (1984).

[20] F. Bechstedt, K. Tenelsen, B. Adolph, and R. Del Sole, Phys. Rev. Lett. **78**, 1528 (1997).

[21] S. L. Adler, Phys. Rev. **126**, 413 (1962).

[22] N. Wiser, Phys. Rev. **129**, 62 (1963).

[23] P. Puschnig and C. Ambrosch-Draxl, Phys. Rev. B **66**, 165105 (2002).

[24] R. W. Godby, M. Schlüter, and L. J. Sham, Phys. Rev. B **37**, 10159 (1988).

[25] C. W. Bunn, Trans. Faraday Soc. **40**, 23 (1944).

[26] D. A. Dows, J. Chem. Phys. **36**, 2836 (1961).

[27] G. Taddei and E. Giglio, J. Chem. Phys. **53**, 2768 (1969).

[28] C.-P. Hsu, S. Hirata, and M. Head-Gordon, J. Phys. Chem. A **105**, 451 (2001).

[29] B. Kohler, Chem. Rev. **93**, 41 (1993).

[30] R. McDiarmid, Int. J. Quantum Chem. **29**, 875 (1986).

[31] H. K. and C. Ambrosch-Draxl, Phys. Rev. B **72**, 205205 (2005).

[32] J. P. Perdew, K. Burke, and M. Ernzerhof, Phys. Rev. Lett. **77**, 3865 (1996).

[33] L. Kleinman and D. M. Bylander, Phys. Rev. Lett. **48**, 1425 (1982).

[34] H. J. Monckhorst and J. D. Pack, Phys. Rev. B **13**, 5188 (1976).

[35] G. R. Elliott and G. E. Leroi, J. Chem. Phys. **59**, 1217 (1973).